

Supporting Information for: Seasonal variations and controlling factors of nitrogen fluxes at the sediment-water interface in a semi-enclosed inland sea

Zhaosen Wu^{1, 2}, Xinyu Guo^{2, *}, Jie Shi^{1, 3}, Xiaokun Ding⁴, Masatoshi Nakakuni^{5, 6},
Kuninao Tada^{5, 6}

¹Key Laboratory of Marine Environment and Ecology, Ministry of Education of China, Ocean University of China, 238 Songling Road, Qingdao 266100, China

²Center for Marine Environmental Studies, Ehime University, 2-5 Bunkyo-Cho, Matsuyama 790-8577, Japan

³Laboratory for Marine Ecology and Environmental Sciences, Qingdao National Laboratory for Marine Science and Technology, Qingdao, 266071, China

⁴School of Ocean, Yantai University, Yantai, 264005, China

⁵Faculty of Agriculture, Kagawa University, Ikenobe, Kita, Miki, Kagawa 761-0701, Japan

⁶Seto Inland Sea Regional Research Center, Kagawa University, Saiwai, Takamatsu, Kagawa 761-0016, Japan

Corresponding to: Xinyu Guo (guo.xinyu.mz@ehime-u.ac.jp) ORCID: 0000-0002-4832-8625

The supplementary material is available, including: Text S1-S5; Figures S1–S5.

Supplementary Text

Text S1 Sensitivity analysis of the sediment model parameters

To evaluate parameter importance, most parameters (Table 2) in the model—whose specific values have not been reported for the Seto Inland Sea—were individually perturbed by $\pm 20\%$, and the relative sensitivity of seven major model outputs was calculated. Figure S1 presents the results. The horizontal axis represents the major model responses, including particulate organic nitrogen (PON) inventory, NH_4^+ inventory, NO_3^- inventory, PON flux, NH_4^+ flux, NO_3^- flux, and N-loss flux, while the vertical axis lists the corresponding model parameters. Each cell reflects the magnitude of sensitivity of a given output to a specific parameter, with both the size and color of the marker indicating the value of the relative sensitivity index. The sensitivity was quantified using

$$E_i = \frac{\Delta Y_j / Y_j}{\Delta X_i / X_i}$$

which represents the proportional change in output (Y_j) resulting from a proportional perturbation in the parameter (X_i).

The results indicate that the model is particularly sensitive to the sinking rate of particulate matter in the water (w) and the critical bottom stress (τ_c). These two parameters directly affect the PON flux across the sediment–water interface. When the bottom shear stress is lower than its critical threshold, the PON flux becomes positively related to the sinking rate, leading to a nearly linear effect on the sedimentary PON inventory. Since PON constitutes the dominant nitrogen pool in sediments, these parameters further extend their influence to other nitrogen species through PON mineralization.

By contrast, the model exhibits relatively low sensitivity to most other parameters. For the majority of parameter–output combinations, the absolute sensitivity values are below 0.2, indicating weak or negligible influence on the modeled nitrogen dynamics. Overall, the sensitivity diagram highlights that only a limited subset of parameters significantly governs model behavior, while most parameters contribute minimally to output variability.

Text S2 Initial concentration of state variables and input profiles in the model

Since more than 99% of total nitrogen (TN) in sediments is particle organic nitrogen (PON), TN concentration profile can be set as PON initial profile¹. The concentration of TN has its maximum value

at the surface of sediment and is almost constant at 50-80 cm, which is treated as the slow-decayed PON for an exponential fitting. The difference between the observed TN and the slow-decayed PON represents the fast-decayed PON.

Ammonium (NH_4^+) concentration profile is constructed by linearly interpolating the observed values. Because of the rapid reduction of nitrate (NO_3^-) concentration to 0 in anaerobic environment, based on the dissolved oxygen (DO) profile, the observed data of the sum of NO_3^- and nitrite (NO_2^-) within the upper 2 cm layer are used for linear fitting as the NO_3^- concentration profile.

The NO_2^- concentration profile is derived as the difference between the observed total oxidized nitrogen concentration (the sum of NO_3^- and NO_2^-) and the NO_3^- concentration profile. Moreover, the model also uses DO concentration and porosity profile data as input for calculation, as shown in Figure S2, in which DO concentration exists in the surface 2 mm layer of sediment.

Text S3 Seasonal variations of nitrogen processes in the sediment

The seasonal variation of mineralization rate of PON in the sediment is controlled by bottom water temperature. The bottom water temperature also affects the nitrification rate by controlling NH_4^+ inventory in the sediment. Similarly, the seasonal variation of the denitrification rate is the same as that of NO_3^- inventory in the sediment. The much greater inventory of NH_4^+ relative to nitrite ensures that the anammox rate is not limited by NH_4^+ and varies little with time. In the anoxic part of the sediment, NO_3^- concentration was low and induced a slow DNRA rate.

Text S4 Effect of concentration of NO_3^- in the bottom water ($\text{NO}_3^{-\text{bw}}$) on NO_3^- inventory in the sediment

The concentration of $\text{NO}_3^{-\text{bw}}$ affects the sediment nitrogen cycle only through the NO_3^- flux at the sediment-water interface. However, the seasonal variation in NO_3^- flux appears to be mainly driven by bottom water temperature, with little sensitivity to the changes in $\text{NO}_3^{-\text{bw}}$. This is because, for the concentration gradient between bottom water and fluff layer of the sediment, the seasonal variation of NO_3^- concentration in fluff layer, controlled by bottom water temperature, has a much stronger impact than that of $\text{NO}_3^{-\text{bw}}$.

Importantly, the NO_3^- inventory in the sediment is insufficient to sustain the daily NO_3^- flux and nitrification, highlighting its rapid turnover., making it also susceptible to the seasonal variation of concentration of $\text{NO}_3^{-\text{bw}}$. Compared with the annual average concentration of $\text{NO}_3^{-\text{bw}}$, its summer concentration is higher, resulting in a lower NO_3^- flux at the sediment-water interface. The difference between the experiment using the annual mean concentration of $\text{NO}_3^{-\text{bw}}$ and the control one shows a marked increase of NO_3^- concentration in the top 1 cm of sediment during summer. Therefore, the reduction of NO_3^- flux allows the sediment to preserve more NO_3^- in its pore water and even a slight change in NO_3^- flux has a significant impact on NO_3^- inventory in the sediment. As a result, NO_3^- inventory is affected by the concentration of $\text{NO}_3^{-\text{bw}}$.

Text S5 Dinitrogen gas (N_2) flux in the upper 5 cm of sediment

Limiting the calculation of denitrification and anammox rates to the top 5 cm of sediment reduces the proportion of anammox in total N_2 flux. In the layer of 0-5 cm, the anammox rate is approximately $0.15 \text{ mmol m}^{-2} \text{ d}^{-1}$, accounting for less than 50% of N_2 production during summer. Specifically, the proportion of anammox reaches a minimum of 45% in August and a maximum of 73% in March.

Supplementary Figures

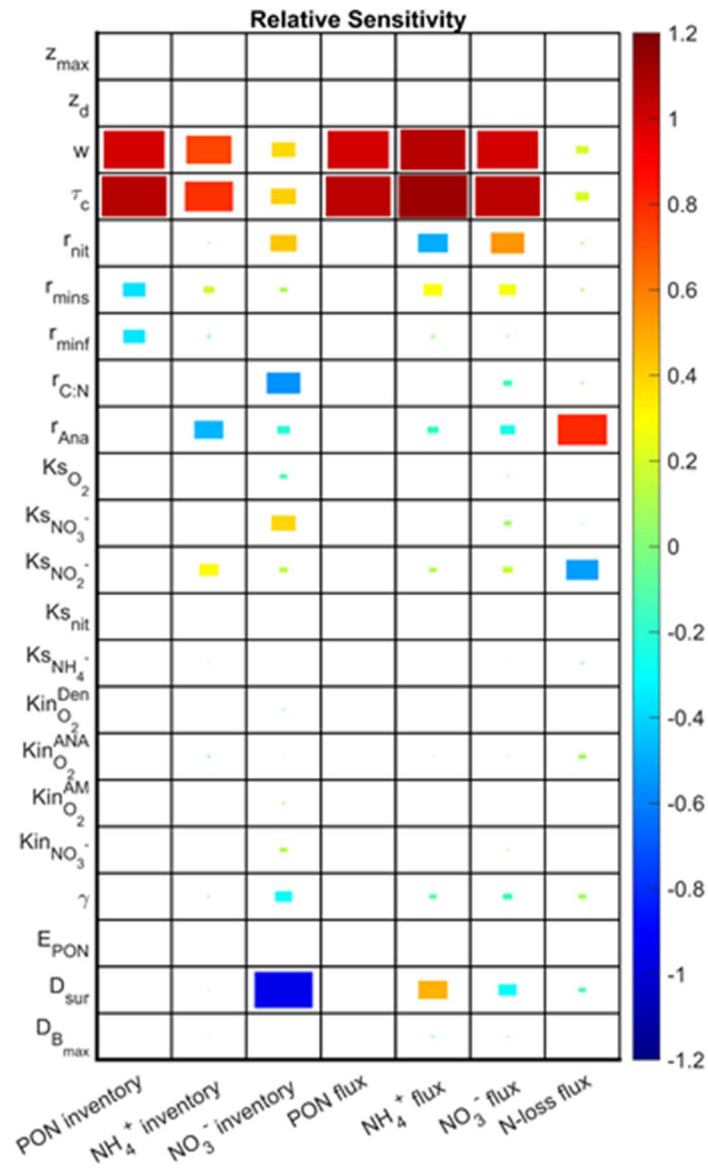


Figure S1. Sensitivity Analysis. The percentage change in the annual average of the main results when the parameter changes by 1%. The expression for relative sensitivity (E_i) is $E_i = \frac{\Delta Y_j / Y_j}{\Delta X_i / X_i}$, where Y_j represents the model results corresponding to the x-axis in the figure, and X_i represents the parameters corresponding to the y-axis in the figure.

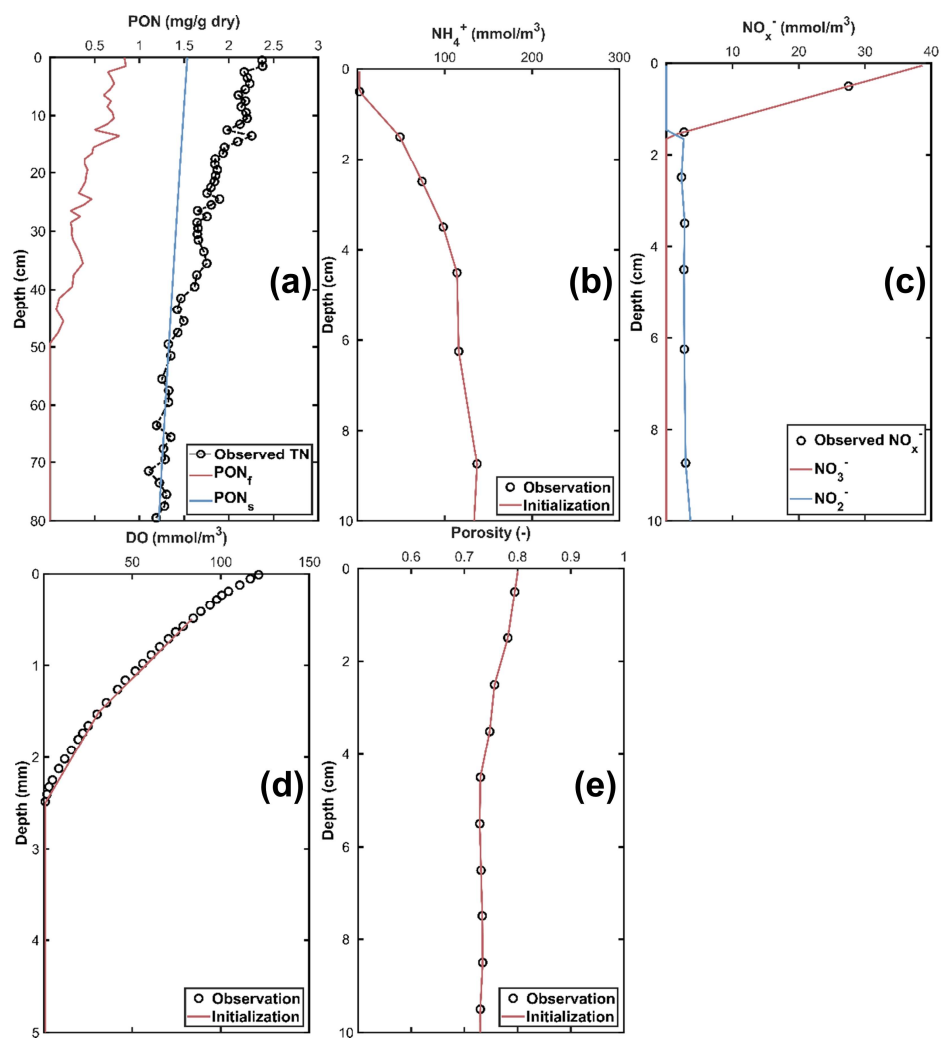


Figure S2. Initial and input profiles for the sediment model: (a) PON; (b) NH_4^+ ; (c) NO_3^- and NO_2^- ; (d) DO; (e) porosity.

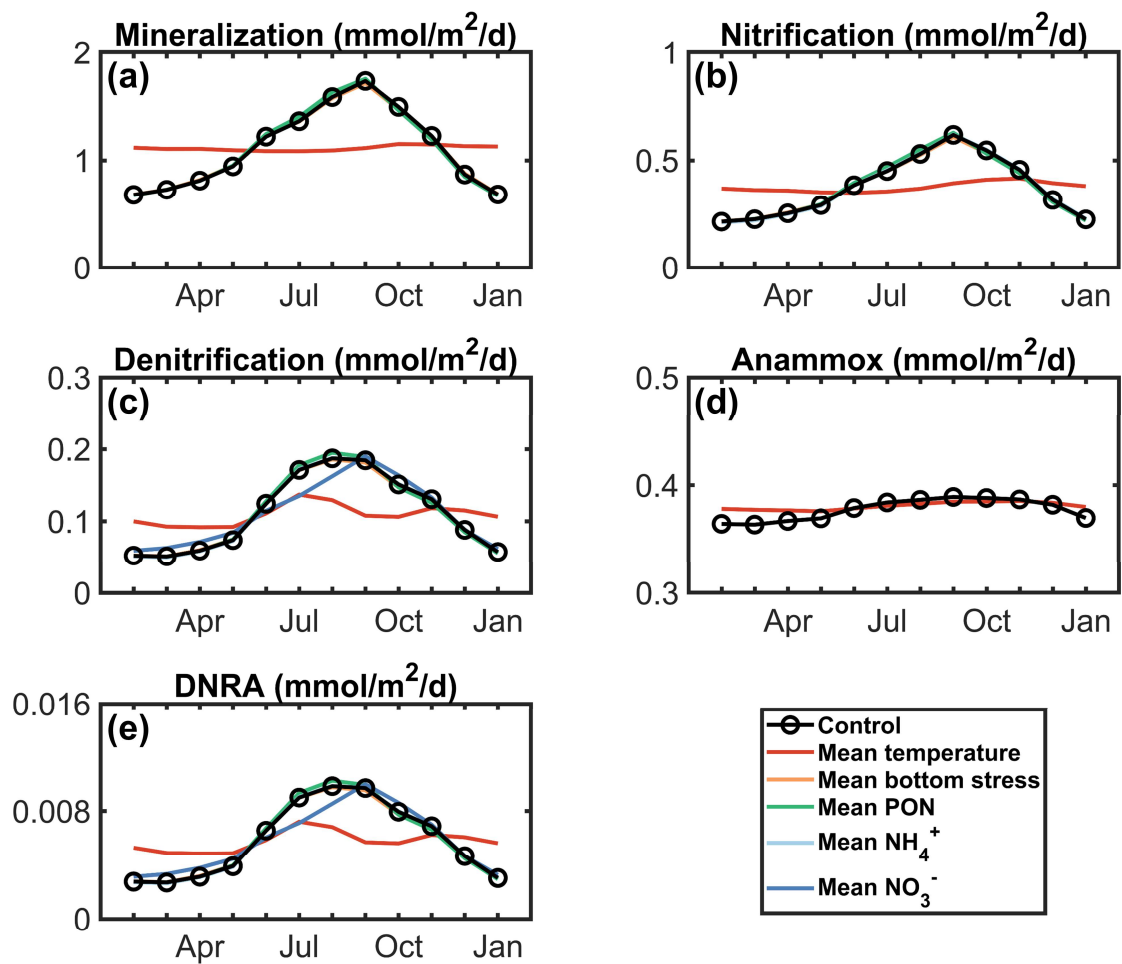


Figure S3. Seasonal variations and the controlled factors of nitrogen reaction rates in the sediment: (a) mineralization; (b) nitrification; (c) denitrification; (d) anammox; (e) DNRA.

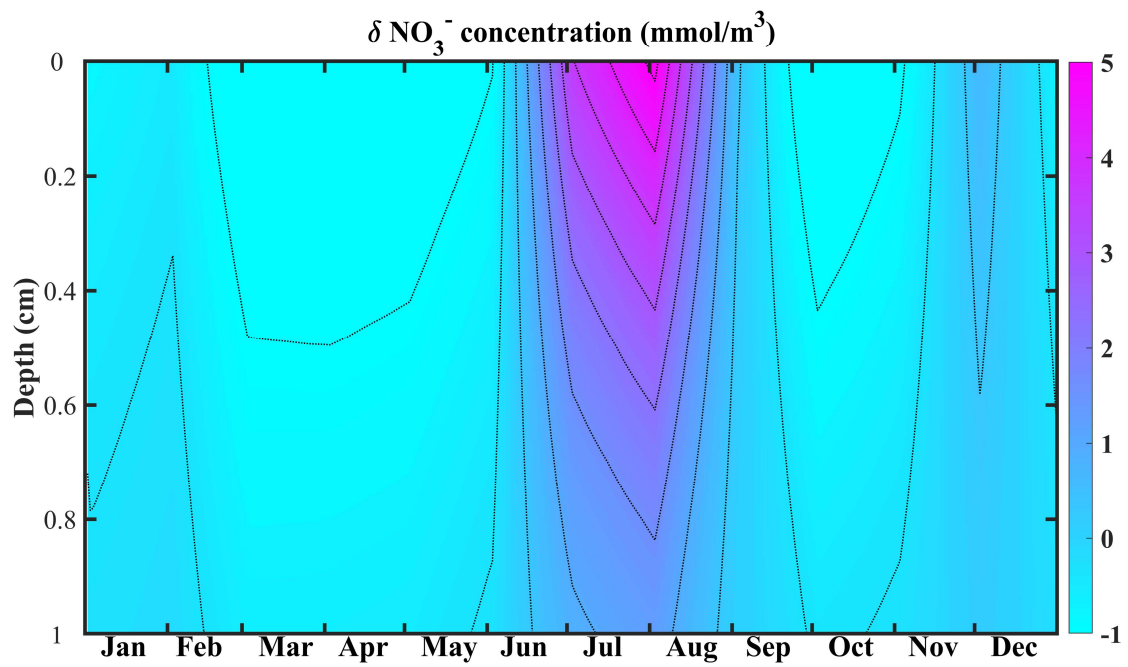


Figure S4. Difference in NO_3^- concentration within the top 1 cm of sediment between the control calculation and the experimental calculation using the annual mean of NO_3^- concentration in the bottom water to replace its monthly values in the control calculation.

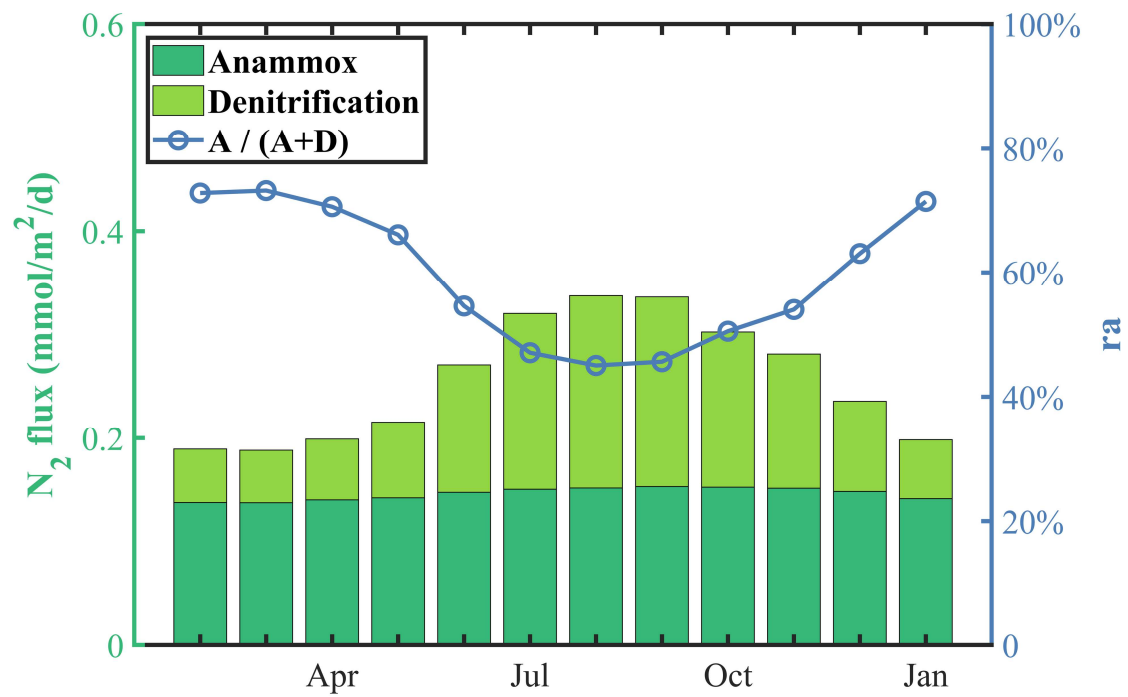


Figure S5. N₂ flux within the top 5 cm of sediment and the ratio of N₂ production by anammox to total N₂ flux (right axis).

References

1. Nakakuni, M.; Yamaguchi, H.; Ichimi, K.; Tada, K., Seasonal variation in pore water nutrients and their fluxes from the bottom sediments in Harima Nada, Seto Inland Sea. *Journal of Oceanography* **2024**, *80*, (3), 219-232.